

INITIATION OF FAILURE IN A SINGLE LAP JOINT

M. BRACCINI¹, M. DUPEUX¹, D. LEGUILLON^{2*}

¹ LTPCM, CNRS UMR 5614, Université Grenoble 1, Saint Martin d'Hères, France.

² LMM, CNRS UMR7607, Université P. et M. Curie, Paris, France.

ABSTRACT

The generalized stress intensity factor (GSIF) criterion is suggested by many authors for the failure prediction at corners in monolithic materials. More recently, it has been successfully used to predict the failure initiation of an adhesive bonding between two steel plates under a 3-point flexion. It involves 2 related critical values. One in the far field takes into account the geometry of the structure but ignores the (small) adhesive thickness. The other in the near field takes into account the adhesive layer but ignores the global structure. Matching conditions ensure the equivalence of these two approaches.

The robustness of the criterion allows using it for the single lap joint failure test as well. The peculiar failure behaviour of this structure is analysed, in a first step for initiation and next for propagation and final failure. The unexpected initiation prediction of the failure mechanism agrees fairly well with a thorough analysis of the experiments.

1 INTRODUCTION

The generalized stress intensity factor (GSIF) criterion

$$k \geq k_c \quad (1)$$

is suggested by many authors for the prediction of crack initiation in V-notched specimens, see for instance Seweryn (1994) [1] and Dunn et al. (1997) [2] and their experiments on PMMA. It has been recently shown (Leguillon 2002 [3]) that the critical value k_c can be expressed in terms of strength σ_c and toughness G_c of the material

$$k_c = \left(\frac{G_c}{K} \right)^{1-\alpha} \sigma_c^{2\alpha-1} \quad (2)$$

where K is a scaling coefficient and α the singularity exponent, both depending only on the notch opening. This expression improves sensibly the Mac Clintock (1958) and Novozhilov (1969) approaches. The agreement with experiments on PMMA (Seweryn 1994 [1], Dunn et al. 1997 [2]) and Alumina (Yosibash et al. 2003 [4]) is good.

More recently, it has been successfully used to predict the failure initiation of an adhesive bonding between two steel plates [5] under a 3-point flexion (figure 1(a)). It involves 2 related critical values. One in the far field takes into account the geometry of the structure but ignores the (small) adhesive thickness. The other in the near field takes into account the adhesive layer but ignores the global structure. Matching conditions ensure the equivalence of these two approaches.

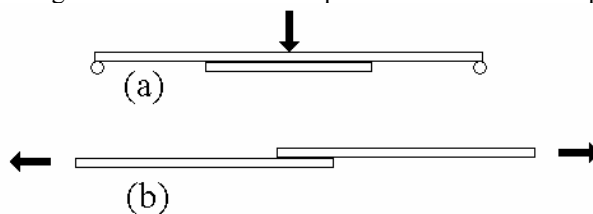


Figure 1: the 3-point bending test (a) and the single lap joint test (b)

The robustness of the criterion allows using it for the single lap joint failure test (figure 1(b)) as well. The peculiar failure behaviour of this structure is analysed, in a first step for initiation and next for propagation and final failure. The unexpected initiation prediction of the failure mechanism agrees fairly well with a thorough analysis of the experiments.

2 THE SINGLE LAP JOINT TEST

Two steel plates $140 \times 25 \times 1$ (mm) are bonded together using an epoxy resin. The plates are cut from 304 stainless steel sheets ($E_1 = 200$ GPa, $\nu_1 = 0.3$). The epoxy resin is the CIBA Araldite 2015 adhesive ($E_2 = 2$ GPa, $\nu_2 = 0.36$). The contact zone is 15 mm long and the adhesive thickness $e = 60$ μm . The testing device allows setting samples so that the two steel plates are pulled in parallel planes. The length of jaws is 75 mm.

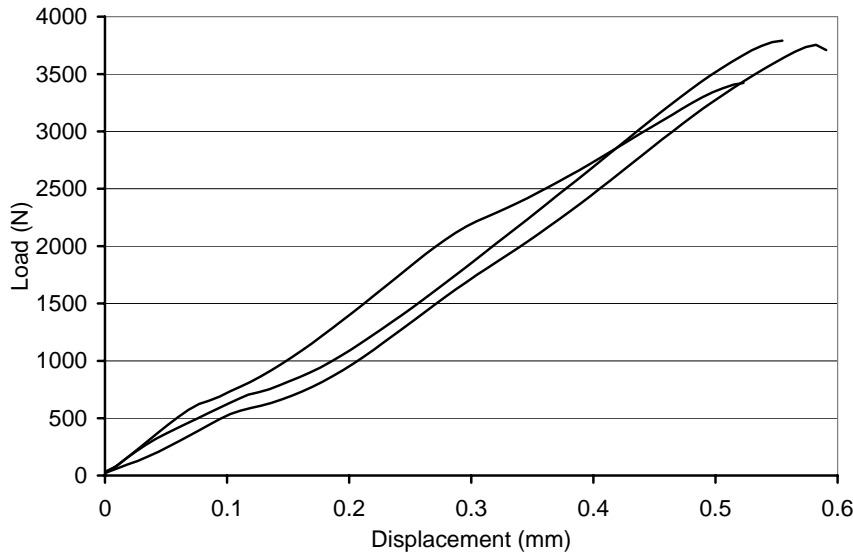


Figure 2: Load/displacement plot for three single lap joint specimens

3 THE ASYMPTOTICS OF THE PROBLEM

The model is based on a two-scale analysis, the small parameter being the adhesive thickness e . At the macro-scale, the adhesive thickness is ignored ($e = 0$) and the two plates are considered as perfectly bonded with continuous displacements and forces (far field). Near the corner between the two steel plates (figure 3(a)), the solution is singular and expands in power terms (x_1, x_2 are the Cartesian coordinates and r, θ the polar ones)

$$\underline{U}^0(x_1, x_2) = \underline{U}^0(0,0) + k r^\alpha \underline{u}(\theta) + \dots \quad (3)$$

α is the singular exponent: $\alpha = 0.545$ at a right angle in a homogeneous material (steel, figure 3(a)), $\underline{u}(\theta)$ is the associated mode and k is the generalized stress intensity factor.

The actual solution (with the index e to recall the dependence on the adhesive thickness) writes

$$\underline{U}^e(x_1, x_2) = \underline{U}^0(x_1, x_2) + \text{small correction} \quad (4)$$

Stretching the domain by $1/e$ (i.e. $y_i = x_i/e$, $\rho = r/e$) and considering the limit $e \rightarrow 0$ leads to an unbounded domain that ignores the global geometry of the specimen. The dimensionless adhesive thickness in this domain is 1. The actual solution expands as

$$\underline{U}^e(x_1, x_2) = \underline{U}^e(e y_1, e y_2) = \underline{U}^0(0, 0) + k e^\alpha \underline{V}(y_1, y_2) + \dots \quad (5)$$

It is a consequence of the matching conditions between the two representations (4) and (5) of the unique actual solution $\underline{U}^e(x_1, x_2)$. In particular $\underline{V}(y_1, y_2)$ must behave like $\rho^\alpha u(\theta)$ at infinity. Indeed, $\underline{V}(y_1, y_2)$ is solution to an elastic problem and undergoes a singular behaviour at the corner between steel and epoxy (near field)

$$\underline{V}(y_1, y_2) = \underline{V}(0, 0) + \kappa \rho^\beta \underline{v}(\theta) + \dots \quad (6)$$

Here $\beta = 0.670$ and κ is independent of the geometry of the specimen and the applied load. It depends only on the elastic contrast between steel and epoxy and is computed once for all $\kappa = 0.29$ (Leguillon et al. 2003 [5]). Then, using (5) and (6), the true intensity factor K of the β singularity in the actual solution is

$$K = k e^{\alpha-\beta} \kappa \quad (7)$$

The failure initiation criterion at the corner (1) writes either $k > k_c$ or $K > K_c$ and the critical values k_c and K_c are related through (7). Failure analysis can be carried out either at the macro or micro scales. The two approaches are equivalent thanks to (7) once again.

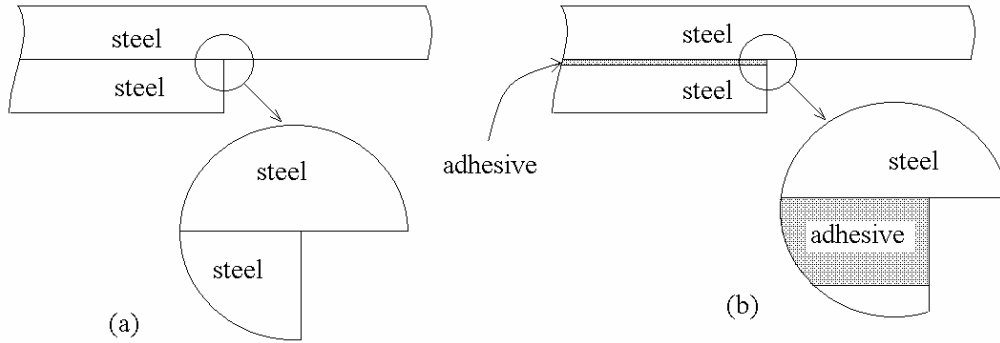


Figure 3: The corner at the macro (a) and micro (b) scales

4 THE SINGLE LAP JOINT FAILURE

In the 3-point bending test, a computation at the macro-scale associated with the (average) failure load gives $k_c = 45.6 \text{ MPa}\cdot\text{mm}^{1-\alpha}$ and following (7) $K_c = 18.8 \text{ MPa}\cdot\text{mm}^{1-\beta}$ (Leguillon et al. 2003 [5]). Failure initiation in the single lap joint is expected to occur for neighbouring values.

The average peak load in figure 2 is $F_{peak} = 3641 \text{ N}$ and, in a first step, it was assumed that crack initiation and final failure coincide. Unfortunately, using this value as the failure load, a numerical simulation of the single lap joint shear test gives a disappointingly high value $k_c' = 80.3 \text{ MPa}\cdot\text{mm}^{1-\alpha}$. A rapid conclusion would be that the failure criterion (1) fails since the expected load corresponding to the critical value k_c estimated in the 3-point bending test would be $F_{ini} = 2068 \text{ N}$, far below the measured peak value.

By chance, a movie was recorded during one of the tests and a thorough analysis shows that a short crack ($\approx 0.5 \text{ mm}$) appears suddenly at the corner, roughly in the middle of the loading phase (figure 4 (a) and (b)). The film is made of 75 pictures, the short crack appears between picture 34 (figure 4 (a)) and picture 35 (figure 4 (b)). The corresponding load is then estimated to be $F_{exp} =$

1795 N, leading to $k_c' = 39.6 \text{ MPa}\cdot\text{mm}^{1-\alpha}$. Predicted F_{mi} and measured F_{exp} loads for crack initiation at the corner are now in a better agreement (<15%).

Next, this short crack no longer grows, up to the final failure starting on picture 71. At peak load, i.e. at the final failure, the computed intensity factors at the tip of the short (0.5 mm) crack are $k_I = 3.1 \text{ MPa}\cdot\text{m}^{1/2}$ and $k_{II} = 3.8 \text{ MPa}\cdot\text{m}^{1/2}$. They correspond to a crack in a homogeneous material (far field). They are related to the true complex intensity factor of the interface crack between the upper steel plate and the adhesive through a similar relation to (7) (Suo, Hutchinson 1989 [6], Leguillon et al. 2003 [5]). To ensure the energy balance, the energy release rate must be the same in the two approaches (near and far fields), the toughness of the interface is then derived from the above data: $G_c(\psi) = 108 \text{ J}\cdot\text{m}^{-2}$ ($\psi = 51^\circ$ is the mode mixity). This is consistent with the toughness obtained in the 3-point bending experiments on pre-cracked specimens (Leguillon et al. 2003 [5]) $G_c(\psi) = 90 \text{ J}\cdot\text{m}^{-2}$ for $\psi = 40^\circ$. The Hutchinson and Suo formula (Hutchinson, Suo 1992 [7]) gives

$$G_c(\psi) = G_{ic} (1 + (1 - \lambda) \tan^2(\psi)) \text{ with } \lambda = 1/2$$

The ratio is 0.77 on one side and 0.83 on the other (<8%).

Finally, the intensity factors and the energy release rate remain almost constant (a slow decay is numerically observed) as the crack length increases. It means that when the macro failure starts it goes on but not in a very brutal way.

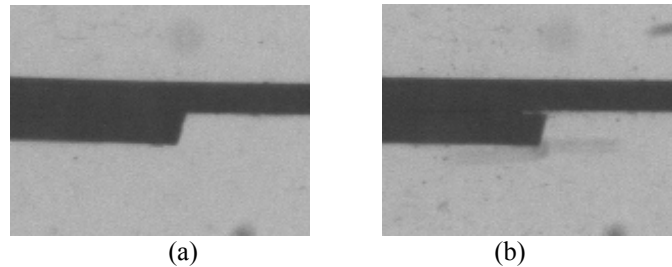


Figure 4: The corner prior to (a) and after (b) the short crack initiation in the single lap joint

5 CONCLUSION

The criterion seems to be enough robust to give satisfying predictions for the crack initiation at a corner between two bonded plates, for different geometries of specimens and different loading modes. The prediction for the single lap joint was not obvious, the initiation does not coincide with the final failure, it occurs almost early during the loading phase. Just after crack initiation (i.e. $F_{exp} = 1795 \text{ N}$), the energy release rate at the tip is $G = 53 \text{ J}\cdot\text{m}^{-2}$, far below the toughness of the interface ($G_c(\psi) = 108 \text{ J}\cdot\text{m}^{-2}$), the short crack cannot propagate until the load is substantially increased.

All these observations are finally in a good agreement with the assumption (initiation is a brutal mechanism), with the prediction of the GSIF criterion for crack initiation, and with the usual fracture mechanics for crack propagation.

REFERENCES

- [1] Seweryn A. (1994) Brittle fracture criterion for structures with sharp notches, Engng. Fract. Mech., 47(5), 673-681.
- [2] Dunn M.L., Suwito W., Cunningham S. (1997) Fracture initiation at sharp notches: correlation using critical stress intensities, Int. J. Solids and Structures, 29(4), 465-501.

- [3] Leguillon D. (2002) Strength or toughness ? A criterion for crack onset at a notch, *Eur. J. of Mechanics – A/Solids*, 21, 61-72.
- [4] Yosibash Z., Bussiba A., Gilad I. (2003) Failure criteria for brittle elastic materials, *Int. J. of Fracture*, 125, 3-4, 307-333.
- [5] Leguillon D., Laurencin J., Dupeux M. (2003) Failure of an epoxy joint between two steel plates, *Eur. J. of Mech. A/Solids*, 22(4), 509-524.
- [6] Suo Z., Hutchinson J.W. (1989) Sandwich test specimens for measuring interface crack toughness, *Mater. Sci. Engng.*, A107, 135-143.
- [7] Hutchinson J.W. Suo Z. (1992) Mixed mode cracking in layered materials, *Advances in Appl. Mech.*, 29, 63-191.